

Error correcting 2D-3D cascaded network for myocardial infarct scar segmentation on late gadolinium enhancement cardiac magnetic resonance images

Matthias Schwab^{a,*}, Mathias Pammeringer^a, Christian Kremser^a, Daniel Obmann^b, Markus Haltmeier^b, Agnes Mayr^a

^aDepartment of Radiology, Medical University of Innsbruck, Innsbruck, 6020, Tirol, Austria

^bDepartment of Mathematics, University of Innsbruck, Innsbruck, 6020, Tirol, Austria

Abstract

Late gadolinium enhancement (LGE) cardiac magnetic resonance (CMR) imaging is considered the in vivo reference standard for assessing infarct size (IS) and microvascular obstruction (MVO) in ST-elevation myocardial infarction (STEMI) patients. However, the exact quantification of those markers of myocardial infarct severity remains challenging and very time-consuming. As LGE distribution patterns can be quite complex and hard to delineate from the blood pool or epicardial fat, automatic segmentation of LGE CMR images is challenging. In this work, we propose a cascaded framework of two-dimensional and three-dimensional convolutional neural networks (CNNs) which enables to calculate the extent of myocardial infarction in a fully automated way. By artificially generating segmentation errors which are characteristic for 2D CNNs during training of the cascaded framework we are enforcing the detection and correction of 2D segmentation errors and hence improve the segmentation accuracy of the entire method. The proposed method was trained and evaluated in a five-fold cross validation using the training dataset from the EMIDEC challenge. We perform comparative experiments where our framework outperforms state-of-the-art methods of the EMIDEC challenge, as well as 2D and 3D nnU-Net. Furthermore, in extensive ablation studies we show the advantages that come with the proposed error correcting cascaded method.

Keywords: Late Gadolinium enhancement, Segmentation, CNN, Infarction

1. Introduction

Although mortality has been declining over the past decades, ischemic heart disease remains the primary cause of death worldwide, being responsible for an estimated 9.1 million global deaths in 2019 (Nowbar et al., 2019; Vos et al., 2020). After ST-segment elevation myocardial infarction (STEMI), the assessment of infarct size is critical for prognosis of major adverse cardiovascular events (MACE) (Larose et al., 2010) and for clinical decision making prior revascularisation. (Kim et al., 2000; Gerber et al., 2012). Furthermore, microvascular obstruction (MVO) was identified as prognostic factor independent of infarct size after reperfused STEMI (de Waha et al., 2017). Cardiac magnetic resonance (CMR) late gadolinium enhancement (LGE) imaging is the reference standard for imaging of ischemic myocardial damage and microvascular obstruction (Kramer et al., 2020). However, in order to obtain these important biomarkers, segmentation of LGE CMR images is necessary, as illustrated in Figure 1.

Different methods for manual or semi-automated LGE quantification on LGE images have been proposed. Manual LGE segmentation by an expert reader is time consuming and requires particular training with limited reproducibility (Flett et al., 2011). Semi-automated meth-

ods for LGE quantification rely on placement of a region of interest (ROI) either in the remote myocardium for the signal threshold versus reference mean (STRM) method, also referred to as the standard deviation (SD) method, or in the infarcted myocardium for the full-width at half-maximum (FWHM) method (McAlindon et al., 2015). Although aiming at reproducibility, ROI placement and size strongly influence signal-intensity thresholds for semi-automated methods (Heiberg et al., 2022). Therefore, fast and reproducible methods for LGE and MVO segmentation after STEMI are desirable.

To circumvent the necessity of manually drawn ROIs, extended intensity based methods have been proposed. Frequently they were based on Otsu thresholding (Tao et al., 2010) or clustering (Detsky et al., 2009). Also fitting myocardial tissue intensities to expected distributions using Gaussian mixture models was proposed (Engblom et al., 2016; Liu et al., 2017). In general these intensity based methods have not achieved clinical adoption as these frameworks do not incorporate any spacial context and hence are very sensitive to noise or imaging artifacts.

As in recent years convolutional neural networks (CNNs) have become state-of-the-art in many image segmentation problems they were also increasingly used in LGE segmentation (Zabihollahy et al., 2018; Moccia et al., 2019; Fahmy et al., 2020). Recently the topic received even more attention, as two challenges were held in the course of the MIC-

*Corresponding author: E-mail: matthias.schwab@i-med.ac.at;

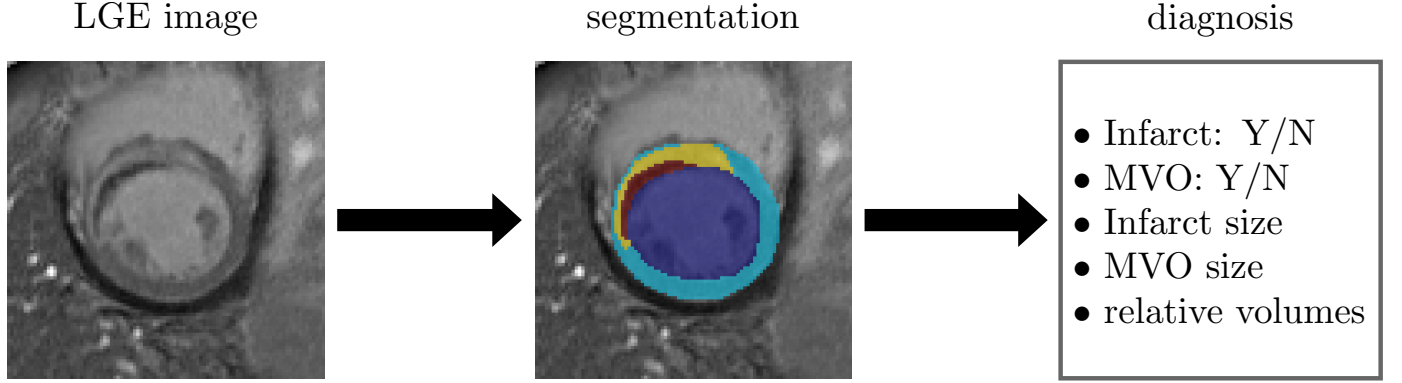


Figure 1: Evaluation of myocardial injury after infarction using LGE CMR. In the short axis images of the left ventricle the tissue gets divided into blood pool (blue) healthy myocardium (cyan), scar tissue (yellow) and MVO (red). Using this segmentation important biomarkers like infarct size or MVO size can be calculated which help to improve clinical decision making as well as predictability for subsequent MACE.

CAI conference in 2020. This included a multi-sequence CMR based myocardial pathology segmentation challenge (Zhuang and Li, 2020; Li et al., 2023) with the goal of combining multi-sequence CMR data (bSSFP, LGE and T2 CMR) to segment different aspects of ischemic myocardial pathology, including normal myocardium, infarction and edema. Another open-source dataset was made available as part of the EMIDEC challenge (Lalande et al., 2020, 2022), a segmentation contest to compare the performance of automatic methods on the segmentation of the myocardium for LGE CMR exams.

More recently, several research works have been focusing on also including prior knowledge into their segmentation method. This was done by incorporating shape, anatomical, spacial or classification prior information into the segmentation frameworks (Yue et al., 2019; Zhou et al., 2021; Brahim et al., 2022; Popescu et al., 2022). Furthermore, also cascaded pipelines have proven to get quite popular lately and have shown good results (Zabihollahy et al., 2020; Zhang, 2021; Lustermaans et al., 2022).

The U-Net architecture (Ronneberger et al., 2015) and its extensions have become one of the most popular architectures for biomedical image segmentation and are also widely used for LGE segmentation. For segmentation of three-dimensional biomedical data usually the 3D U-Net is the more suitable method, since it is able to extract volumetric information in all spacial directions and hence is usually outperforming its two-dimensional counterpart, which focuses only on intra-slice information. However, the voxel spacing of the 3D volumes in LGE CMR images usually is highly anisotropic. For example in the EMIDEC dataset the median voxel spacing is $1.458\text{mm} \times 1.458\text{mm} \times 10\text{mm}$. This means that the resolution in x and y direction is almost 7 times higher than in z direction and hence treating the three axis all equally is far from optimal. Therefore, Zhang (2021) proposed a cascaded pipeline trying to combine the strengths of two and three-dimensional segmentation methods. In our opinion, the main advantage of this method is not that the 2D network

can better process the intra-slice information but the fact that errors made by the 2D method on a full MR volume are quite characteristic due to its two-dimensional structure. We therefore claim that it is possible to detect and improve these 2D-characteristic errors with a 3D network. If, for example, the 2D segmentation in one single slice deviates very strongly from the neighboring ones, there is a relatively high probability that an error is present in this slice. However, when training a 2D-3D cascaded framework such characteristic errors are quite rare since the performance of the 2D network was optimized on the same training dataset. We therefore propose to include artificially created 2D-characteristic segmentation errors during training of the cascaded framework. This strengthens the ability of the resulting method to detect and correct 2D-segmentation errors which further improves the generalizability properties of the method on unseen data. By constructing characteristic 2D segmentation mistakes we implicitly include prior information into our method. For example deleting LGE segmentation in one random slice of the 3D volume can be interpreted as implicitly including prior information about the three-dimensional structure of the segmentation objects.

To summarize the main contributions of this work are as follows:

- We present a novel perturbation module for efficient training of cascaded 2D-3D segmentation pipelines, which improves the generalization properties of the final method to unseen data.
- We test our method on the public EMIDEC dataset and show that we outperform current state-of-the-art methods regarding different segmentation metrics.
- We conduct extensive ablation experiments and investigate the effects of the cascaded pipeline and perturbation module on the segmentation accuracy.

The rest of the paper is organized as follows. Section 2 describes the proposed error-correcting segmenta-

tion framework for automated scar pattern detection in LGE CMR volumes. In Section 3, the experimental results achieved on the EMIDEC dataset are presented. Section 4 discusses results, limitations and potential directions for future works. Finally, Section 5 gives a short summary of the presented research.

2. Material and methods

2.1. Dataset

For this work the publicly available LGE CMR database from the EMIDEC challenge (Lalande et al., 2022) was used. All together this dataset consists of 150 clinical exams containing healthy patients (1/3) and patients with myocardial infarction (2/3). Each exam includes a series of LGE CMR images in short axis orientation covering the left ventricle from the base to the apex. The CMR acquisition was performed on 1.5T and 3T Siemens MRI scanners at the University Hospital of Dijon (France). All measurements were performed ECG-gated and were carried out 10 minutes after gadolinium based contrast agent injection using a T1-weighted phase sensitive inversion recovery (PSIR) sequence (TR = 3.5 ms, TE = 1.42 ms, TI = 400 ms, flip angle = 20). The data were divided into training ($n = 100$) and testing ($n = 50$) datasets where ground truth segmentation masks were only provided for patients in the training set. The manual delineations were outlined by two experts (a cardiologist with 10 years of experience and a biophysicist with 20 years of experience) and include the endocardial and epicardial borders, the infarcted areas as well as the areas of MVO, if present. To summarize, the ground truth annotations divide the images into five different classes: blood pool, healthy myocardium, myocardial scar, MVO and background. Exact details on the EMIDEC dataset can be found in Lalande et al. (2020).

2.2. Preprocessing

Since the EMIDEC dataset exclusively includes CMR slices in which myocardium is present, and the center of gravity of the left ventricle is realigned to the center of each image, no extensive preprocessing pipeline is necessary. To get a bigger proportion of foreground pixels per sample the original input images are cropped to 96×96 pixels around the center of the left ventricle. After that all the images are normalized independently to have zero mean and a standard derivation of one. For the three dimensional stack an input size of $96 \times 96 \times 7$ is chosen. For volumes containing more than 7 slices this is achieved by randomly selecting subvolumes of 7 contiguous slices during training. For examinations containing less than 7 MR slices the volume is resized using nearest neighbor interpolation with respect to the z -axis.

2.3. Network architecture

The main architecture of our method consists of a cascade of 2D and 3D U-Nets. The framework can therefore be divided into two main steps.

1. Segmentation on the individual slices of the CMR volume by a two-dimensional CNN.
2. Refinement of the 2D segmentation masks with the help of a three-dimensional CNN.

For both networks we use basic U-Net architectures (Ronneberger et al., 2015) with kernel sizes of 3×3 and $3 \times 3 \times 3$, respectively. After each convolutional block we apply instance normalization followed by a leaky rectified linear unit (ReLU) activation function. For the 2D U-Net downsampling is achieved by max-pooling and upsampling by bilinear interpolation. The 3D U-Net uses strided convolutions, following Szegedy et al. (2016), for downsampling as well as strided convolution transposed for upsampling. Since the image size is already very small in the third dimension no downsampling or upsampling is performed regarding this dimension resulting in feature sizes of $6 \times 6 \times 7$ at the bottleneck of the network. To prevent the 3D method from merely copying the segmentation masks provided by the 2D network, we only add the 2D segmentation masks for infarction and MVO as additional input, leaving segmentation of healthy myocardium and blood pool to the 3D network alone. The overall configuration of our framework is illustrated in Figure 2.

2.4. Postprocessing

To be able to objectively assess the influence of different methods on the final segmentation result we refrain from any postprocessing steps. We simply take the argmax over the different segmentation channels as our final class prediction. After that we zero pad the predicted segmentation masks to bring them back to the original field-of-view.

2.5. Data augmentation

To provide a stream of constantly changing training examples we apply various data augmentation techniques during training. This includes intensity based transformations such as Gaussian blurring, gamma correction, additive white noise, changing contrast and brightness as well as simulating images with lower resolution. In addition to this we also use various geometric transformations including translation, flipping, elastic deformation and scaling to further improve the data variety during training.

2.6. Perturbation module

One of the main advantages of the cascaded pipeline is that potential segmentation errors done in the first stage can be corrected afterwards. However, one big issue arising during training is that the coarse segmentation masks provided as additional input are already quite precise, since

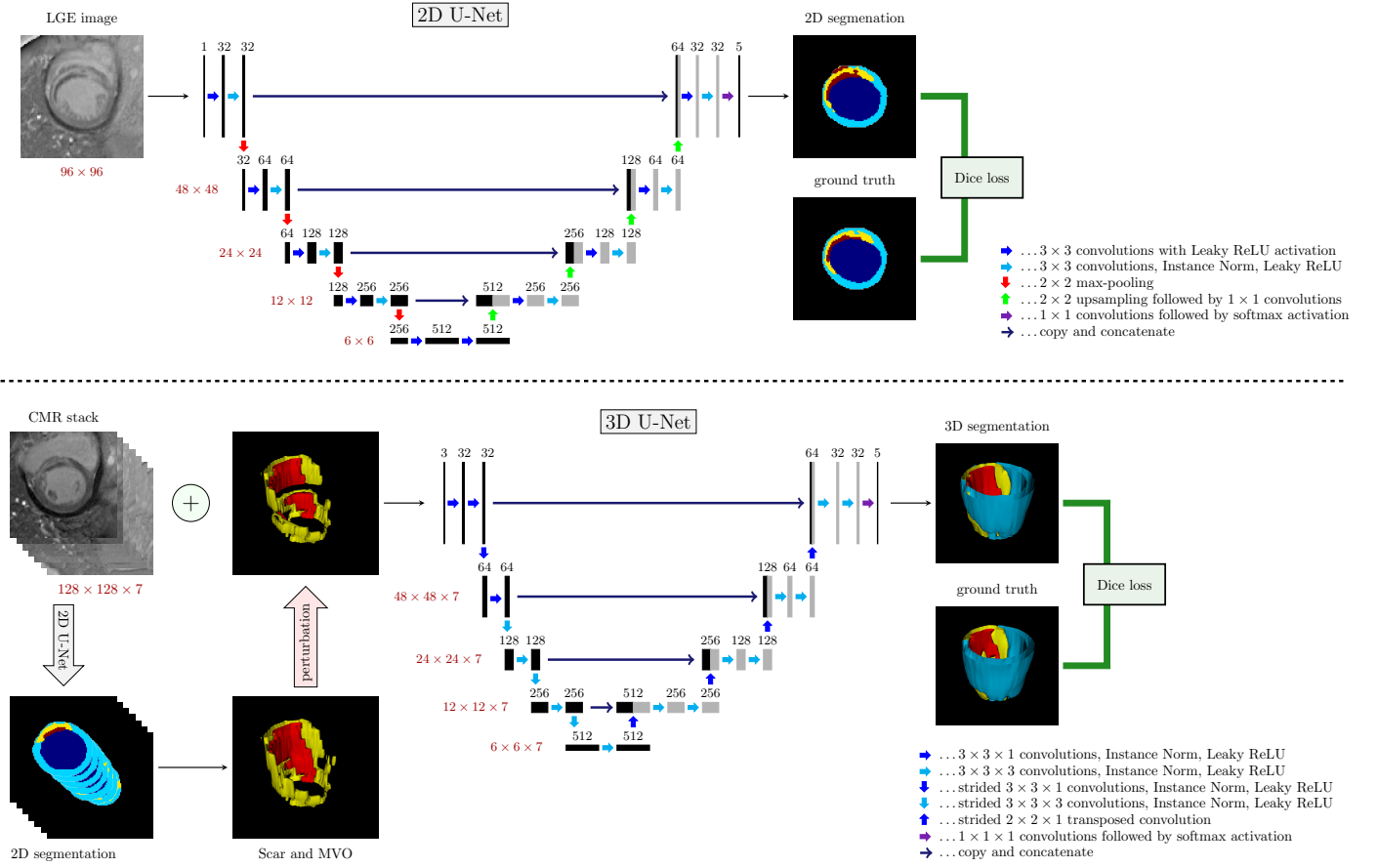


Figure 2: The proposed segmentation pipeline. Firstly a 2D U-Net is trained on the individual images of the training dataset. After that a 3D U-Net is trained to refine the segmentation and return the final three-dimensional segmentation volume for the left ventricle. Input for the 3D CNN are the LGE CMR volumes as well as the possibly perturbed segmentation masks for scar and MVO provided by the pre-trained 2D CNN.

2D-net was optimized on the same training dataset. Therefore, we introduce a novel perturbation module which ensures that segmentation errors made by the first network due to missing information about neighboring slices are detected and improved by the subsequent network.

The idea is to artificially create different 2D-characteristic segmentation errors during training in order to then allow the 3D network to learn to correct them. This includes:

- Slightly increasing some data augmentation parameters compared to the 2D augmentation pipeline. More precisely this means increasing the ranges from which contrast, brightness and gamma augmentations get chosen as well as producing images of even lower resolution.
- Randomly deleting the 2D segmentations for a specific class (myocardial scar or MVO or both) on single slices (see Figure 3 second and third row).
- Adding wrong annotations for infarction to single slices. If this is triggered for a sample a random slice of the 3D-volume is chosen and the 85th percentile

of the pixel values of the myocardium in this slice is calculated using the ground truth segmentation mask. After thresholding regarding this percentile we add the biggest connected component as scar to this specific slice (see Figure 3 first row).

- Adding wrong MVO annotations to single slices. Since MVO always occurs inside an infarcted region, we are generating fake MVO annotations by randomly choosing a pixel which was classified by the 2D framework as scar and change the label of this pixel as well as a few random neighboring pixels to MVO (see Figure 3 fourth row).
- Setting the whole 2D-segmentation mask to zero for some random samples.

During training of the cascaded pipeline at most one of these operations is chosen randomly with small probabilities. Since most of the perturbations are performed only in single slices of the whole MR volume, the three-dimensional system is specially trained to detect errors that are characteristic for missing inter-slice information.

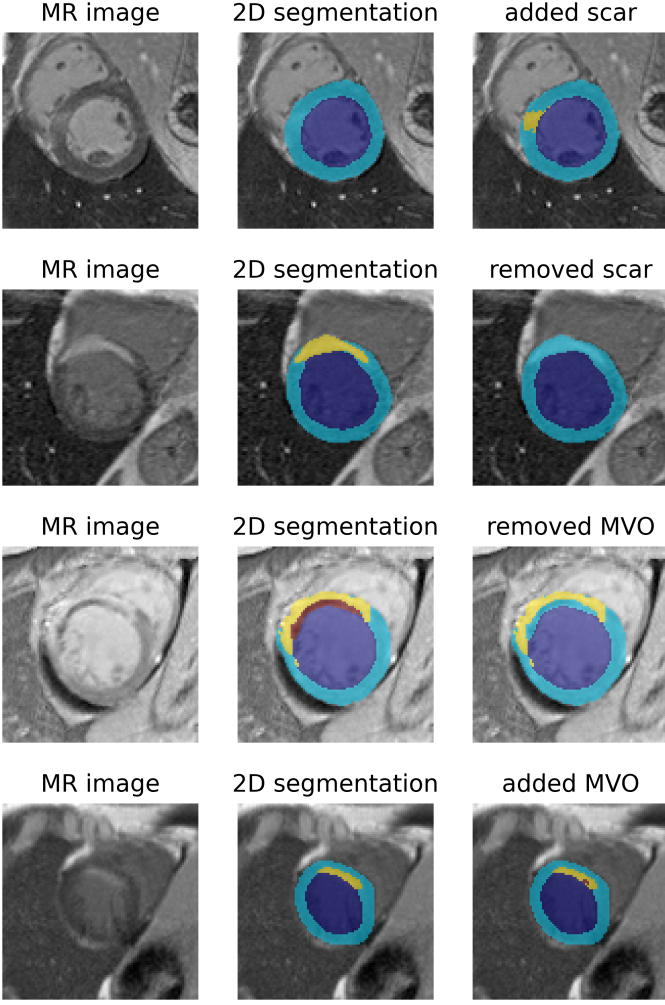


Figure 3: Examples for the artificial modifications of the 2D segmentation masks. The first row shows an example where the 2D segmentation correctly segmented a healthy patient, however, an artificial scar was created by the perturbation module. Row two shows a contrary example where scar tissue was at first correctly identified but was removed afterwards. Rows three and four show examples for removed resp. added MVO segmentation.

By introducing this kind of perturbations during training we enforce the 3D network to be nearly invariant under erroneous 2D segmentations in single slices. To illustrate this let us denote $(x_i)_{i=1}^M$ as the three dimensional input stack of the CMR, where M is the number of 2D slices for the specific examination. Further we denote the CNNs as ϕ_{2D} and ϕ_{3D} , respectively. Now let δ_k be a perturbation operator, which is acting on the k -th slice of a segmentation mask. By training our cascaded framework on disturbed as well as on clean segmentation masks we guide the three dimensional framework to have the property

$$\begin{aligned} \phi_{3D}((x_i)_{i=1}^M, \delta_k((\phi_{2D}(x_i))_{i=1}^M)) \\ \simeq \phi_{3D}((x_i)_{i=1}^M, (\phi_{2D}(x_i))_{i=1}^M). \end{aligned} \quad (1)$$

Interpreting δ_k as a 2D segmentation error happening in the k -th slice of the CMR volume Equation 1 shows the

capability of the cascaded framework for correcting segmentation errors on single slices.

2.7. Loss

As loss function a variation of the Dice loss (Equation 2) as proposed in Milletari et al. (2016) was used. As this loss is equivalent to the negative Dice coefficient for binary images, its main advantage is that it is very useful for establishing the right balance between foreground and background voxels. This enables us to get rid of assigning weights to samples of different classes. Therefore, for all the foreground classes (blood pool, healthy myocardium, scar, MVO) during training we minimize

$$L_{DCE} = -\frac{2 \sum_{i \in I} p_i g_i}{\sum_{i \in I} p_i^2 + \sum_{i \in I} g_i^2}, \quad (2)$$

where I is the set of pixels, $p \in \mathbb{R}^I$ is the networks segmentation prediction and $g \in \{0, 1\}^I$ is the corresponding ground truth mask. To alleviate the common problem of “vanishing gradients” we use deep supervision (Lee et al., 2015) additionally providing direct supervision to some hidden layers instead of only supervising the output layer.

The detailed training procedure looks as follows. At first we trained the two-dimensional U-Net with a batch size of 32 over 750 epochs. Then the 3D cascade framework was trained for 750 epochs using a batch size of 4. When training the 3D cascade, the perturbation module was switched on after 100 training epochs to further enforce the detection and improvement of 2D segmentation errors of the final method. For minimization of the loss, stochastic gradient descent with Nesterov momentum ($\mu = 0.99$) and initial learning rate of 0.005 (2D) and 0.01 (3D), respectively was used. All the training of the framework was performed on a NVIDIA A40 GPU using the Pytorch deep learning library.

2.8. Reference methods

We compare our method against three other approaches which we briefly describe in this section.

- **nnU-Net** (Isensee et al., 2021) is a deep learning based segmentation framework for biomedical images. It is a self-configuring method which has proven to be state-of-the-art in biomedical image segmentation on a wide variety of different datasets and is very commonly used as a baseline method. At MICCAI 2020, for example, 9 out of 10 challenge winners built their methods on top of nnU-Net. Since the method can handle different image dimensions, we compare our method to both 2D and 3D nnU-Net.
- Since we use the data set of the EMIDEC Challenge in this paper, we also compare our method with that of the **winner of the challenge** (Zhang, 2021). Similar to us, this method uses a cascaded

Table 1: Results of the five-fold cross-validation for the proposed method.

Targets	Metrics	Fold 1	Fold 2	Fold 3	Fold 4	Fold 5	Mean	SD
Myocardium	DSC(%)	87.24	86.20	87.00	85.12	85.11	86.13	0.9
	AVD(mm ³)	8289	8761	6920	8037	12105	8823	1749
	HAUS(mm)	13.95	12.78	11.39	13.50	17.46	13.82	2.02
Infarction	DSC(%)	76.54	70.64	79.75	77.70	75.54	76.03	3.04
	AVD(mm ³)	2904	5391	2054	3853	5847	4010	1439
	AVDR(%)	2.45	3.83	1.76	3.23	4.49	3.15	0.97
MVO	DSC(%)	69.33	76.27	83.66	78.33	57.72	73.06	8.94
	AVD(mm ³)	759	1580	877	356	953	905	395
	AVDR(%)	0.64	1.03	0.63	0.35	0.70	0.67	0.22

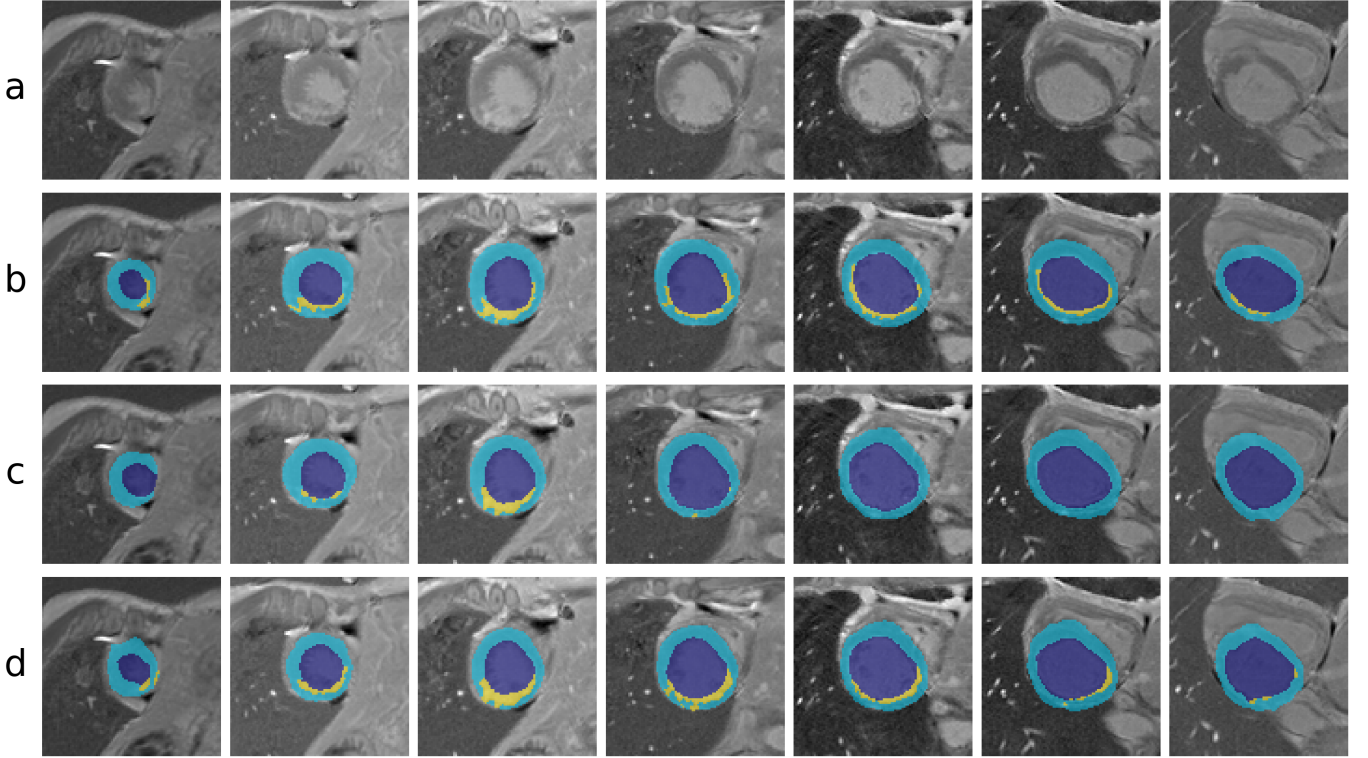


Figure 4: Example of an LGE CMR stack (a) with according manual segmentation (b). Scar tissue is missed by the 2D method (c) in some slices. The cascaded method (d) is able to improve the segmentation performance, correctly identifying additional scar tissue in neighboring slices.

pipeline for image segmentation, where simply the full 2D segmentations are added as additional channels to a 3D network without any special attention to whether this information is used or not for the final prediction.

2.9. Evaluation metrics

To quantify the segmentation accuracy of our method we stick to the metrics proposed by the organizers of the EMIDEC challenge, which incorporates both clinical and geometrical metrics. For the evaluation of the myocardial tissue this includes Dice coefficient (DSC), Hausdorff-distance (HAUS) in mm as well as absolute volume difference (AVD) in mm³. The Dice coefficient (Equation 3) is

a measure of the spacial overlap between two sets P and G . It is defined as

$$\text{DSC} = \frac{2|P \cap G|}{|P| + |G|}, \quad (3)$$

where $|\cdot|$ denotes the cardinality of a set. In our case P presents the final segmentation prediction of our method and G the manual gold standard. The range of the Dice coefficient resides between 0 (no overlap at all) and 1 (perfect match). The Hausdorff-distance (Equation 4) also is a common metric evaluating the degree of mismatch between two segmentation boundaries by calculating Euclidean distances. It is defined as

$$\text{HAUS} = \max\{\max_{p \in P} d(p, G), \max_{g \in G} d(g, P)\}, \quad (4)$$

Table 2: A comparison of evaluation scores of different methods on a five-fold cross-validation on the EMIDEC dataset. Best values are marked in bold.

Targets	Metrics	2D nnU-Net	3D nnU-Net	Zhang (2021)	Ours
Myocardium	DSC(%)	85.50	87.21	87.15	86.13
	AVD(mm ³)	7564	6879	6474	8823
	HAUS(mm)	27.96	14.16	14.04	13.82
Infarction	DSC(%)	50.85	72.95	72.08	76.03
	AVD(mm ³)	5610	4469	4179	4010
	AVDR(%)	4.53	3.57	3.41	3.15
MVO	DSC(%)	67.35	71.36	71.01	73.06
	AVD(mm ³)	1058	969	919	905
	AVDR(%)	0.78	0.71	0.69	0.67

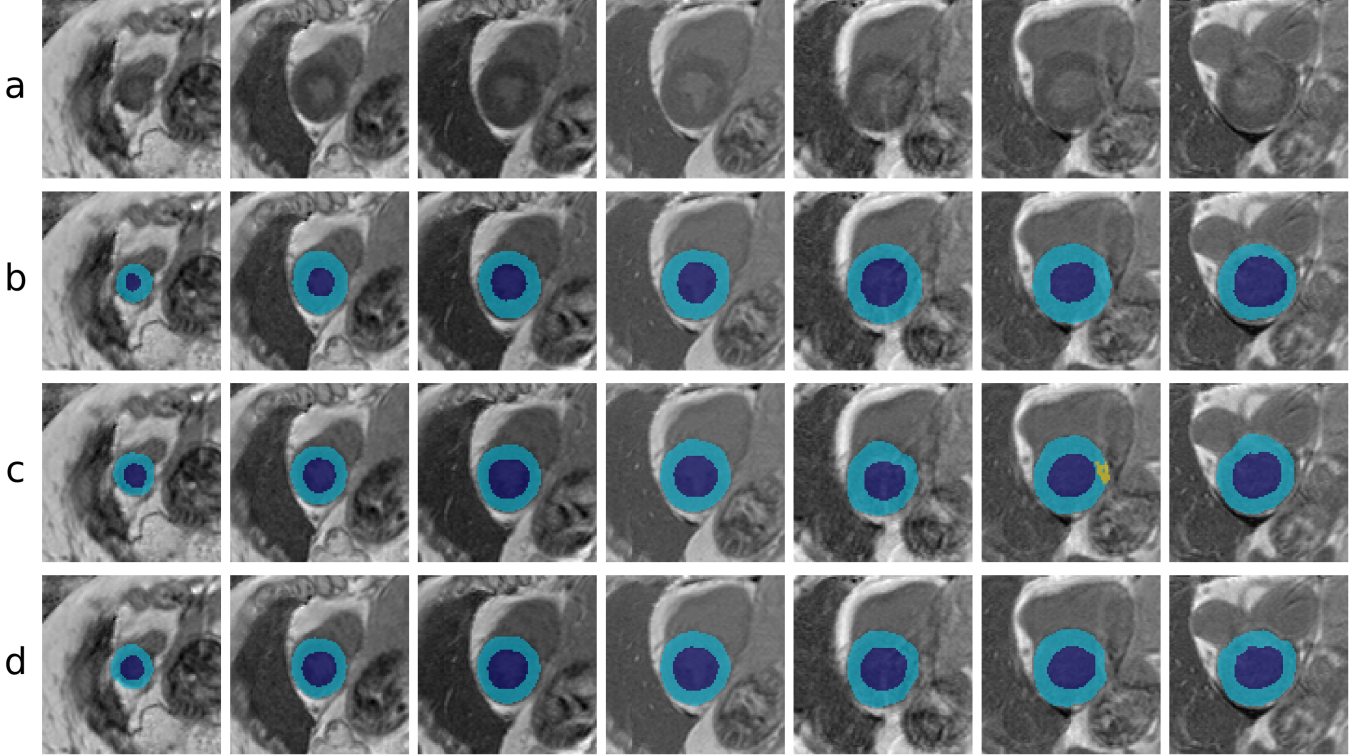


Figure 5: Example of a healthy patient. The wrongly identified scar tissue gets recognized and removed by the cascaded pipeline. (a) LGE MR image, (b) ground truth, (c) 2D segmentation, (d) 3D cascade segmentation.

where $d(a, B) = \min_{b \in B} \|a - b\|$ quantifies the minimal euclidean distance from a point $a \in A$ to set B . Further, the absolute volume difference (Equation 5) calculates the amount of difference between the volume V_A obtained by the proposed method and the volume V_M calculated from the manual segmentations

$$AVD = |V_A - V_M|. \quad (5)$$

For quantification of infarction and MVO volumes additionally the absolute volume difference rate (AVDR) according to the volume of the myocardium, which we denote by V_{MYO} , is calculated (Equation 6). To ensure consistency with the results of the reference methods, the evaluation scores were calculated using the official eval-

uation code of the EMIDEC challenge (<https://github.com/EMIDEC-Challenge/Evaluation-metrics/>).

$$AVDR = \frac{AVD}{V_{MYO}}. \quad (6)$$

3. Experiments and results

3.1. Five-fold cross validation

To test the performance of our method, we split the 100 exams of the dataset where there are ground truth labels available into five random subsets and performed a five-fold cross validation. So for each fold we have 80 exams available for training and 20 exams for evaluation.

Table 3: Ablation study on five-fold cross-validation. Comparing mean Dice coefficients of the different methods. Best values are marked in bold.

Methods	Myocardium	Infarction	MVO
2D U-Net	85.35	68.81	71.71
3D U-Net	85.27	72.26	71.13
vanilla cascade	86.61	72.25	72.83
Ours	86.13	76.03	73.06

The results that our method achieved on the different folds are displayed in Table 1. Taking the mean over all folds we achieved Dice coefficients of 86% for the entire myocardium, 76.03% for infarcted tissue and 73.06% for MVO. The mean Hausdorff distance between predicted and ground truth myocardium was 13.82mm³ and the average AVDR with respect to myocardial volume was 3.15% for infarction and 0.67% for MVO, respectively. Also the standard deviations (SD) between the results on the different folds are displayed in Table 1.

3.2. Reference methods

We further compared the proposed method to the reference methods described in Section 2.8. The mean values considering the five-fold cross validation regarding the different metrics are displayed in Table 2. For infarction and MVO our method outperforms the reference methods in all three metrics. Considering the Dice coefficients of MI segmentation our method performed significantly better than 2D nnU-Net ($p < 0.001$) using a Wilcoxon signed-rank test. Considering the segmentation of myocardium all four methods performed very similar with Dice coefficients ranging between 85.5% (2D nnU-Net) and 87.21% (3D nnU-Net). Regarding Dice scores of MVO segmentation, differences between the methods were slightly larger, albeit non-significant. However, clearly the biggest performance differences between the methods was found for the segmentation of infarcted tissue. Here the mean Dice coefficients range from 50.85% (2D nnU-Net) to 76.03% (proposed method) as illustrated in Table 2.

3.3. Ablation studies

To investigate the impact of the individual steps of the whole pipeline we also performed ablation studies. We compared the performance of our proposed cascaded method with that of simple 2D and 3D U-nets, respectively. Furthermore, we investigated the influence of the perturbation module by training exactly the same cascaded pipeline with the only difference that during training the 2D segmentation masks of scar and MVO were passed unchanged to the 3D U-Net. We refer to this method as “vanilla cascade”. Table 3 displays the mean Dice coefficients of the different methods for myocardium infarction and MVO achieved on a five-fold cross validation study. Regarding myocardium and MVO all the methods perform

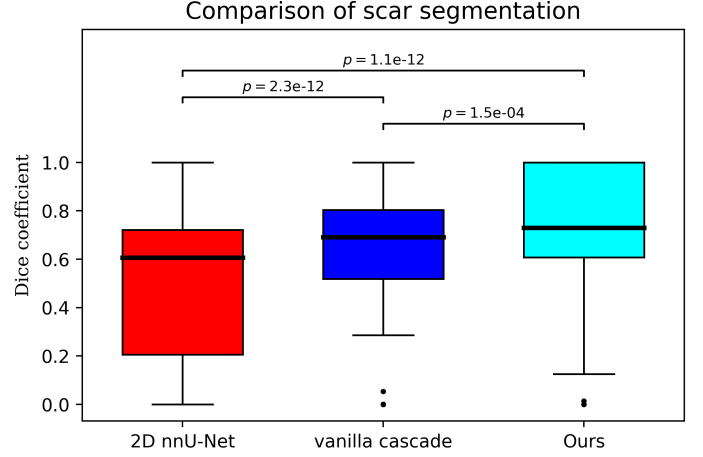


Figure 6: Box plots of Dice coefficients for scar segmentation comparing 2D nnU-Net, vanilla cascade framework and our proposed method.

approximately equally well. However, for the segmentation of myocardial infarction the mean Dice coefficient increased from 68.81% for 2D U-Net to 72.26% when using 3D U-Net. Also the vanilla cascaded framework produced very similar results as the single 3D U-Net (mean Dice coefficient of 72.25%). Regarding infarction our proposed framework achieved a Dice score of 76.03%, which is significantly higher than all other approaches also including the vanilla cascaded framework ($p = 0.03$). In terms of MVO, the proposed method also achieved the highest dice values, but here no significant difference could be found compared to the other methods.

To further test how well the proposed framework is able to correct 2D segmentation errors we investigated the performance of the cascaded pipeline when using the predictions of 2D nnU-Net. As shown in Table 4 the segmentation of infarction is not very precise when using 2D nnU-Net only resulting in a mean Dice score of 50.85%. When further applying the cascaded framework to refine this segmentations mean Dice coefficient increased to 62.01%. Finally when using our cascade network which was trained using the perturbation module the Dice coefficient further improves to 71.12%. Box plots for the Dice coefficients regarding segmentation of MI for the three different frameworks are shown in Figure 6. The proposed framework also showed the best results regarding AVD (4097mm³) and AVDR (3.25%). For MVO segmentation the cascaded framework also improved segmentation performance (see Table 5). However, the improvement was much smaller than for the scar segmentation (mean DCE of 67.35% for 2D nnU-Net compared to 69.65% for vanilla cascade). The results for MVO segmentation achieved by our proposed method compared to the vanilla cascaded framework were basically the same for all three metrics.

Table 4: A comparison study of evaluation scores regarding segmentation of MI when using 2D nnU-Net, cascaded method as well as our proposed method. Best values are marked in bold.

Methods	DSC(%)	AVD(mm ³)	AVDR(%)
2D nnU-Net	50.85	5610	4.53
vanilla cascade	62.01	4624	3.72
Ours	71.12	4097	3.25

Table 5: A comparison study of evaluation scores regarding segmentation of MVO when using 2D nnU-Net, cascaded method as well as our proposed method. Best values are marked in bold.

Methods	DSC(%)	AVD(mm ³)	AVDR(%)
2D nnU-Net	67.35	1058	0.78
vanilla cascade	69.65	978	0.73
Ours	69.55	982	0.73

4. Discussion

In this work an error correcting 2D-3D cascade framework for myocardial scar segmentation on LGE CMR images was introduced. Using both 2D and 3D segmentation methods this approach is able to optimally combine their strengths. By at first training on two dimensional images the advantage that there are much more 2D images than 3D volumes available for training is used. After that, the three-dimensional CNN exploits both the relationships between the slices as well as preceding 2D segmentations. By introducing various perturbations to the 2D segmentation masks during training we further guide the predictions of the final framework to be invariant under various 2D segmentation errors. The proposed pipeline was trained using images and manual segmentations of the publicly available EMIDEC training dataset.

Our method outperformed state-of-the-art methods in both scar and MVO segmentation. Especially in segmentation of MI our method outperformed other approaches significantly. Compared with the winner of the EMIDEC challenge (Zhang, 2021) we reached an improvement of the Dice score by almost 4% for MI segmentation. Also in MVO segmentation our method performed superior compared to all the reference methods, although the differences did not reach the level of significance. To summarize, our method reached mean Dice scores of 86.13% for myocardium segmentation, 76.03% for scar segmentation and 73.06% for MVO segmentation. This Dice scores are higher than scores reported for inter-observer studies and very similar to intra-observer scores. For example, on a separate test dataset consisting of 34 examinations Lalande et al. (2020) report intra-observer Dice coefficients of 84% for myocardium and 76% for MI segmentation. For the inter-observer study Dice scores were 83% and 69% for the two classes. This shows that our automatic segmentation is of comparable quality to manual segmentation.

A possible disadvantage of cascaded methods is that errors made in the first steps could get propagated through the subsequent steps. This could also be a problem in

the cascade of two and three-dimensional segmentations, since it is also conceivable that structures that were drawn incorrectly by the 2D network are adopted almost one-to-one by the subsequent 3D method. However, our proposed perturbation module that is interposed between 2D output and 3D input during training allows to suppress these propagation of errors. As illustrated in Figure 4, our cascaded method is able to fully detect scars that were only partially detected by the 2D method. On the other hand, the framework is also able to detect incorrectly marked scars on healthy patients due to artifacts or noise and remove them for the final segmentation prediction (see Figure 5). In an ablation study we showed that our method is significantly outperforming single 2D and 3D segmentation methods as well as the vanilla cascade framework. Further, we were able to show that our framework works even when 2D segmentation methods are used, which were not applied during training of the cascaded module indicating the stability of our method. For example, we were able to massively improve the segmentation performance of myocardial infarction of the 2D nnU-Net from a mean Dice score of 50.85% to 71.17%. In addition, the influence of the perturbation module was very clearly demonstrated, as the vanilla cascade framework only improved the mean Dice coefficient to 62%.

Our thorough analysis of the impact of the different parts of the proposed pipeline to the segmentation performance using a challenging dataset with partially noisy images including various artifacts suggests that our framework may also be generally applicable to different applications. In our opinion, our framework can specifically be applied to three-dimensional segmentation problems with anisotropic pixel spacing where there is a limited number of manually segmented 3D volumes available.

Although we were able to significantly improve scar segmentation compared to state-of-the-art methods, regarding MVO the proposed method performs very similar to the reference methods. When comparing the Dice coefficients for MVO segmentation of the different methods no significant differences were found. We suspect that this is the case because MVO is typically a much smaller structure that is not always visible across multiple layers. In the dataset we used there e.g. are examinations in which MVO only appears on one single slice in the whole CMR volume. This leads us to believe that the inclusion of inter slice information unfortunately does not really lead to a massive improvement for MVO segmentation. However, the clinical information that MVO always occurs only within the center of a MI can also be exploited for MVO segmentation. Therefore, including shape priors into the framework, for example using neural networks for shape reconstruction, as proposed by Yue et al. (2019), might be of interest for future work. Another possibility to improve the MVO segmentation could also be to incorporate classification priors to the framework as done by Brahim et al. (2022). By adding a binary classification module to the bottleneck of their segmentation network they were able

to improve their methods accuracy in identifying MVO regions. Therefore, we believe that our method could also benefit from adding such classification priors to 2D or 3D frameworks, which may also be of interest for future work. Another approach to further improve detection of MVO in the future could be to also include clinical information about the patients into the segmentation framework.

A major limitation of this work is that it used a homogeneous cohort of LGE CMR images from a single hospital using uniform imaging protocols as well as scanners from only one single manufacturer. Therefore, it is quite possible that our trained models do not perform as well on different clinical cohorts due to the “domain-shift”. Another limitation is that the EMIDEC dataset we used does not reflect clinical reality. For example, the data contains only slices in which myocardium of the left ventricle is visible. Furthermore, images were registered in such a way that the left ventricle is in the center of each image. However, when dealing with data in a clinical setting this can not be expected. Therefore, to make the method applicable to clinical data, some preprocessing steps would still be necessary. Finally, we also want to mention that we could not test our method on the test dataset of the EMIDEC challenge which contains 50 additional examinations, since the manual labels for these images are not publicly available. This is a further limitation of our work, as an additional evaluation of the results on a separate test dataset would be desirable.

5. Conclusion

In this paper we describe a deep learning-based cascaded framework for a fully automatized segmentation of myocardial tissue in LGE CMR images. With the introduced perturbation module between the two segmentation networks during training our framework is able to detect and correct segmentation errors which happen during the first segmentation step. In a five-fold cross validation study our proposed method outperformed state-of-the-art methods in terms of segmentation accuracy regarding different metrics. Also we showed the positive impact of the newly introduced perturbation module to the segmentation of MI. Additionally our method proved to show myocardium, scar and MVO segmentations that are comparable to the manual segmentations. However, especially in MVO segmentation there is some room for improvement as not all cases of MVO were identified correctly by our method. Thus further studies which integrate prior information such as shape or also clinical metadata information are desirable for future research to further improve the automatic detection of myocardial abnormalities.

Declaration of Competing Interest

Declaration of Competing Interest The authors declare that they have no known competing financial interests or

personal relationships that could have appeared to influence the work reported in this paper.

Acknowledgments

This work was supported by the Austrian Science Fund (FWF) [grant number DOC 110].

CRedit author statement

Matthias Schwab: Methodology, Software, Writing - Original Draft. **Mathias Pamminger:** Writing - Review & Editing, Investigation. **Christian Kremser:** Conceptualization, Writing - Review & Editing. **Daniel Obmann:** Software. **Markus Haltmeier:** Conceptualization, Supervision. **Agnes Mayr:** Project administration, Supervision.

References

- Brahim, K., Arega, T.W., Boucher, A., Bricq, S., Sakly, A., Meriaudeau, F., 2022. An improved 3D deep learning-based segmentation of left ventricular myocardial diseases from delayed-enhancement MRI with inclusion and classification prior information U-Net (ICPIU-Net). *Sensors* 22, 2084. doi:10.3390/s22062084.
- Detsky, J.S., Paul, G., Dick, A.J., Wright, G.A., 2009. Reproducible classification of infarct heterogeneity using fuzzy clustering on multicontrast delayed enhancement magnetic resonance images. *IEEE Transactions on Medical Imaging* 28, 1606–1614. doi:10.1109/TMI.2009.2023515.
- Engblom, H., Tufvesson, J., Jablonowski, R., Carlsson, M., Aletras, A.H., Hoffmann, P., Jacquier, A., Kober, F., Metzler, B., Erlinge, D., Atar, D., Arheden, H., Heiberg, E., 2016. A new automatic algorithm for quantification of myocardial infarction imaged by late gadolinium enhancement cardiovascular magnetic resonance: experimental validation and comparison to expert delineations in multi-center, multi-vendor patient data. *Journal of Cardiovascular Magnetic Resonance* 18, 1–13. doi:10.1186/s12968-016-0242-5.
- Fahmy, A.S., Neisius, U., Chan, R.H., Rowin, E.J., Manning, W.J., Maron, M.S., Nezafat, R., 2020. Three-dimensional deep convolutional neural networks for automated myocardial scar quantification in hypertrophic cardiomyopathy: a multicenter multivendor study. *Radiology* 294, 52–60. doi:10.1148/radiol.2019190737.
- Flett, A.S., Hasleton, J., Cook, C., Hausenloy, D., Quarta, G., Ariti, C., Muthurangu, V., Moon, J.C., 2011. Evaluation of techniques for the quantification of myocardial scar of differing etiology using cardiac magnetic resonance. *JACC: cardiovascular imaging* 4, 150–156. doi:10.1016/j.jcmg.2010.11.015.
- Gerber, B.L., Rousseau, M.F., Ahn, S.A., Le Polain De Waroux, J.B., Pouleur, A.C., Philips, T., Vancraeynest, D., Pasquet, A., Vanoverschelde, J.L.J., 2012. Prognostic value of myocardial viability by delayed-enhanced magnetic resonance in patients with coronary artery disease and low ejection fraction: impact of revascularization therapy. *Journal of the American College of Cardiology* 59, 825–835. doi:10.1016/j.jacc.2011.09.073.
- Heiberg, E., Engblom, H., Carlsson, M., Erlinge, D., Atar, D., Aletras, A.H., Arheden, H., 2022. Infarct quantification with cardiovascular magnetic resonance using “standard deviation from remote” is unreliable: validation in multi-centre multi-vendor data. *Journal of Cardiovascular Magnetic Resonance* 24, 1–12. doi:10.1186/s12968-022-00888-8.
- Isensee, F., Jaeger, P.F., Kohl, S.A., Petersen, J., Maier-Hein, K.H., 2021. nnU-Net: a self-configuring method for deep learning-based biomedical image segmentation. *Nature methods* 18, 203–211. doi:10.1038/s41592-020-01008-z.

- Kim, R.J., Wu, E., Rafael, A., Chen, E.L., Parker, M.A., Simonetti, O., Klocke, F.J., Bonow, R.O., Judd, R.M., 2000. The use of contrast-enhanced magnetic resonance imaging to identify reversible myocardial dysfunction. *New England Journal of Medicine* 343, 1445–1453. doi:10.1056/NEJM200011163432003.
- Kramer, C.M., Barkhausen, J., Bucciarelli-Ducci, C., Flamm, S.D., Kim, R.J., Nagel, E., 2020. Standardized cardiovascular magnetic resonance imaging (CMR) protocols: 2020 update. *Journal of Cardiovascular Magnetic Resonance* 22, 1–18. doi:doi.org/10.1186/s12968-020-00607-1.
- Lalande, A., Chen, Z., Decourselle, T., Qayyum, A., Pommier, T., Lorgis, L., de la Rosa, E., Cochet, A., Cottin, Y., Gin-hac, D., Salomon, M., Couturier, R., Meriaudeau, F., 2020. Emidec: A database usable for the automatic evaluation of myocardial infarction from delayed-enhancement cardiac MRI. *Data* 5. doi:10.3390/data5040089.
- Lalande, A., Chen, Z., Pommier, T., Decourselle, T., Qayyum, A., Salomon, M., Gin-hac, D., Skandarani, Y., Boucher, A., Brahim, K., de Bruijne, M., Camarasa, R., Correia, T.M., Feng, X., Girum, K.B., Hennemuth, A., Huellebrand, M., Hussain, R., Ivantsits, M., Ma, J., Meyer, C., Sharma, R., Shi, J., Tsekos, N.V., Varela, M., Wang, X., Yang, S., Zhang, H., Zhang, Y., Zhou, Y., Zhuang, X., Couturier, R., Meriaudeau, F., 2022. Deep learning methods for automatic evaluation of delayed enhancement-MRI: the results of the EMIDEC challenge. *Medical Image Analysis* 79, 102428. doi:10.1016/j.media.2022.102428.
- Larose, E., Rodés-Cabau, J., Pibarot, P., Rinfret, S., Proulx, G., Nguyen, C.M., Déry, J.P., Gleeton, O., Roy, L., Noël, B., Barbeau, G., Rouleau, J., Boudreault, J.R., Amyot, M., De Larochelière, R., Bertrand, O.F., 2010. Predicting late myocardial recovery and outcomes in the early hours of ST-segment elevation myocardial infarction: traditional measures compared with microvascular obstruction, salvaged myocardium, and necrosis characteristics by cardiovascular magnetic resonance. *Journal of the American College of Cardiology* 55, 2459–2469. doi:10.1016/j.jacc.2010.02.033.
- Lee, C.Y., Xie, S., Gallagher, P., Zhang, Z., Tu, Z., 2015. Deeply-supervised nets, in: *Artificial intelligence and statistics*, PMLR. pp. 562–570. URL: <https://proceedings.mlr.press/v38/lee15a.html>.
- Li, L., Wu, F., Wang, S., Luo, X., Martín-Isla, C., Zhai, S., Zhang, J., Liu, Y., Zhang, Z., Ankenbrand, M.J., Jiang, H., Zhang, X., Wang, L., Arega, T.W., Altunok, E., Zhao, Z., Li, F., Ma, J., Yang, X., Puybareau, E., Oksuz, I., Bricq, S., Li, W., Punithakumar, K., Tsaftaris, S.A., Schreiber, L.M., Yang, M., Liu, G., Xia, Y., Wang, G., Escalera, S., Zhuang, X., 2023. MyoPS: A benchmark of myocardial pathology segmentation combining three-sequence cardiac magnetic resonance images. *Medical Image Analysis* , 102808doi:10.1016/j.media.2023.102808.
- Liu, J., Zhuang, X., Wu, L., An, D., Xu, J., Peters, T., Gu, L., 2017. Myocardium segmentation from DE MRI using multicomponent gaussian mixture model and coupled level set. *IEEE Transactions on Biomedical Engineering* 64, 2650–2661. doi:10.1109/TBME.2017.2657656.
- Lustermans, D.R., Amirrajab, S., Veta, M., Breeuwer, M., Scannell, C.M., 2022. Optimized automated cardiac MR scar quantification with GAN-based data augmentation. *Computer Methods and Programs in Biomedicine* 226, 107116. doi:10.1016/j.cmpb.2022.107116.
- McAlindon, E., Pufulete, M., Lawton, C., Angelini, G.D., Bucciarelli-Ducci, C., 2015. Quantification of infarct size and myocardium at risk: evaluation of different techniques and its implications. *European Heart Journal-Cardiovascular Imaging* 16, 738–746. doi:10.1093/ehjci/jev001.
- Milletari, F., Navab, N., Ahmadi, S.A., 2016. V-net: Fully convolutional neural networks for volumetric medical image segmentation, in: 2016 fourth international conference on 3D vision (3DV), Ieee. pp. 565–571. doi:10.1109/3DV.2016.79.
- Moccia, S., Banali, N., Martini, C., Muscogiuri, G., Pontone, G., Pepi, M., Caiani, E.G., 2019. Development and testing of a deep learning-based strategy for scar segmentation on CMR-LGE images. *Magnetic Resonance Materials in Physics, Biology and Medicine* 32, 187–195. doi:10.1007/s10334-018-0718-4.
- Nowbar, A.N., Gitto, M., Howard, J.P., Francis, D.P., Al-Lamee, R., 2019. Mortality from ischemic heart disease: Analysis of data from the world health organization and coronary artery disease risk factors from NCD risk factor collaboration. *Circulation: cardiovascular quality and outcomes* 12, e005375. doi:10.1161/CIRCOUTCOMES.118.005375.
- Popescu, D.M., Abramson, H.G., Yu, R., Lai, C., Shade, J.K., Wu, K.C., Maggioni, M., Trayanova, N.A., 2022. Anatomically informed deep learning on contrast-enhanced cardiac magnetic resonance imaging for scar segmentation and clinical feature extraction. *Cardiovascular Digital Health Journal* 3, 2–13. doi:10.1016/j.cvdhj.2021.11.007.
- Ronneberger, O., Fischer, P., Brox, T., 2015. U-net: Convolutional networks for biomedical image segmentation, in: *Medical Image Computing and Computer-Assisted Intervention-MICCAI 2015: 18th International Conference, Munich, Germany, October 5-9, 2015, Proceedings, Part III* 18, Springer. pp. 234–241. doi:10.1007/978-3-319-24574-4_28.
- Szegedy, C., Vanhoucke, V., Ioffe, S., Shlens, J., Wojna, Z., 2016. Rethinking the inception architecture for computer vision, in: 2016 IEEE Conference on Computer Vision and Pattern Recognition (CVPR), IEEE. pp. 2818–2826. doi:10.1109/CVPR.2016.308.
- Tao, Q., Milles, J., Zeppenfeld, K., Lamb, H.J., Bax, J.J., Reiber, J.H., Van Der Geest, R.J., 2010. Automated segmentation of myocardial scar in late enhancement MRI using combined intensity and spatial information. *Magnetic Resonance in Medicine* 64, 586–594. doi:doi.org/10.1002/mrm.22422.
- Vos, T., Lim, S.S., Abbafati, C., Abbas, K.M., Abbasi, M., Abbasi-fard, M., Abbasi-Kangevari, M., Abbastabar, H., Abd-Allah, F., Abdelalim, A., et al., 2020. Global burden of 369 diseases and injuries in 204 countries and territories, 1990–2019: a systematic analysis for the global burden of disease study 2019. *The Lancet* 396, 1204–1222. doi:10.1016/S0140-6736(20)30925-9.
- de Waha, S., Patel, M.R., Granger, C.B., Ohman, E.M., Maehara, A., Eitel, I., Ben-Yehuda, O., Jenkins, P., Thiele, H., Stone, G.W., 2017. Relationship between microvascular obstruction and adverse events following primary percutaneous coronary intervention for ST-segment elevation myocardial infarction: an individual patient data pooled analysis from seven randomized trials. *European heart journal* 38, 3502–3510. doi:10.1093/eurheartj/ehx414.
- Yue, Q., Luo, X., Ye, Q., Xu, L., Zhuang, X., 2019. Cardiac segmentation from LGE MRI using deep neural network incorporating shape and spatial priors, in: *Medical Image Computing and Computer Assisted Intervention-MICCAI 2019: 22nd International Conference, Shenzhen, China, October 13–17, 2019, Proceedings, Part II* 22, Springer. pp. 559–567. doi:10.1007/978-3-030-32245-8_62.
- Zabihollahy, F., Rajchl, M., White, J.A., Ukwatta, E., 2020. Fully automated segmentation of left ventricular scar from 3D late gadolinium enhancement magnetic resonance imaging using a cascaded multi-planar U-Net (CMPU-Net). *Medical physics* 47, 1645–1655. doi:10.1002/mp.14022.
- Zabihollahy, F., White, J.A., Ukwatta, E., 2018. Myocardial scar segmentation from magnetic resonance images using convolutional neural network, in: *Medical Imaging 2018: Computer-Aided Diagnosis, SPIE*. pp. 663–670. doi:10.1117/12.2293518.
- Zhang, Y., 2021. Cascaded convolutional neural network for automatic myocardial infarction segmentation from delayed-enhancement cardiac MRI, in: *Statistical Atlases and Computational Models of the Heart. M&Ms and EMIDEC Challenges*, Springer. pp. 328–333. doi:10.1007/978-3-030-68107-4_33.
- Zhou, Y., Zhang, K., Luo, X., Wang, S., Zhuang, X., 2021. Anatomy prior based U-Net for pathology segmentation with attention, in: *Statistical Atlases and Computational Models of the Heart. M&Ms and EMIDEC Challenges*, Springer. pp. 392–399. doi:10.1007/978-3-030-68107-4_41.
- Zhuang, X., Li, L., 2020. Multi-sequence CMR based myocardial pathology segmentation challenge. doi:10.5281/zenodo.3715932.